

THE COMMUNITY EARTH SYSTEM MODEL

A Framework for Collaborative Research

BY JAMES W. HURRELL, M. M. HOLLAND, P. R. GENT, S. GHAN, JENNIFER E. KAY, P. J. KUSHNER, J.-F. LAMARQUE, W. G. LARGE, D. LAWRENCE, K. LINDSAY, W. H. LIPSCOMB, M. C. LONG, N. MAHOWALD, D. R. MARSH, R. B. NEALE, P. RASCH, S. VAVRUS, M. VERTENSTEIN, D. BADER, W. D. COLLINS, J. J. HACK, J. KIEHL, AND S. MARSHALL

By simulating biogeochemical cycles, the Greenland ice sheet, and more—with reach to the lower thermosphere—this system gives the research community a flexible, state-of-the-science tool for understanding climate variability and change.

The National Center for Atmospheric Research (NCAR) has a proud history of strong collaboration with scientists from universities, national laboratories, and other research organizations to develop, document, improve, and support the scientific use of a comprehensive modeling system that is at the forefront of international efforts to understand and predict the behavior of Earth's climate. For many years this tradition has been realized through the development and application of the Community Climate System Model (CCSM; Blackmon et al.

2001). Several versions of the CCSM have been used in many hundreds of peer-reviewed studies to better understand climate variability and climate change. In addition, simulations performed with CCSM have made a significant contribution to both national and international assessments of climate, including those of the Intergovernmental Panel on Climate Change (IPCC) and the U.S. Global Change Research Program (USGCRP). The CCSM thus provides the broader academic community with a core modeling system for multiple purposes.

AFFILIATIONS: HURRELL, HOLLAND, GENT, KAY, LAMARQUE, LARGE, LAWRENCE, LINDSAY, LONG, MARSH, NEALE, VERTENSTEIN, AND KIEHL—National Center for Atmospheric Research,* Boulder, Colorado; GHAN AND RASCH—Pacific Northwest National Laboratory, Richland, Washington; KUSHNER—Department of Physics, University of Toronto, Toronto, Ontario, Canada; LIPSCOMB—Los Alamos National Laboratory, Los Alamos, New Mexico; MAHOWALD—Cornell University, Ithaca, New York; VAVRUS—University of Wisconsin—Madison, Madison, Wisconsin; BADER—Lawrence Livermore National Laboratory, Livermore, California; COLLINS—Lawrence Berkeley National Laboratory, University of California, Berkeley, Berkeley, California; HACK—Oak Ridge National

Laboratory, Oak Ridge, Tennessee; MARSHALL—University of Calgary, Calgary, Alberta, Canada

*The National Center for Atmospheric Research is sponsored by the National Science Foundation.

CORRESPONDING AUTHOR: J. W. Hurrell, NCAR Earth System Laboratory, P.O. Box 3000, Boulder, CO 80307-3000
E-mail: jhurrell@ucar.edu

The abstract for this article can be found in this issue, following the table of contents.

DOI:10.1175/BAMS-D-12-00121.1

In final form 30 November 2012
©2013 American Meteorological Society

The most recent version of the model [CCSM, version 4 (CCSM4)] was released to the community on 1 April 2010. Gent et al. (2011) documented CCSM4 and summarized developments to all of the model components as well as described its major simulation characteristics relative to those of CCSM, version 3 (CCSM3; Collins et al. 2006). Many other aspects of fully coupled simulations performed with CCSM4, ranging from paleoclimate to future climate runs, are documented in the CCSM4/CESM1 (version 1.0 of the Community Earth System Model) special collection of the *Journal of Climate* (see <http://journals.ametsoc.org/page/CCSM4/CESM1>).

There is no unique definition of which processes must be represented before a climate model becomes an Earth system model (ESM), but typically such models have at least an interactive carbon cycle component (Flato 2011). The development of this capability was motivated by suggestions that the ability of terrestrial ecosystems and the ocean to remove carbon dioxide from the atmosphere will be limited by future climate change (e.g., Friedlingstein et al. 2006). There are now a significant number of ESMs in use by the international research community—for instance, those developed at the Met Office Hadley Centre (Collins et al. 2011), the Geophysical Fluid Dynamics Laboratory (Dunne et al. 2012), and the Max Planck Institute for Meteorology (Giorgetta et al. 2013), to name just a few.

In parallel with the development of CCSM4, additional capabilities, leading to what has become CESM1, were added in order to address a wider range of pressing scientific questions. These capabilities included interactive carbon–nitrogen cycling, global dynamic vegetation and land use change due to human activity, a marine ecosystem–biogeochemical module, and new chemical and physical processes to study both the direct and indirect effects of aerosols on climate. The atmospheric chemistry component was updated, and the model can be run with a “high top” atmosphere that extends from the surface to the thermosphere [the Whole Atmosphere Community Climate Model (WACCM); Marsh et al. 2013] in order to better understand the role of the upper atmosphere in climate variability and change. Also, a land ice component can be coupled to simulate changes to the Greenland Ice Sheet and its role in future climate change.

The release of CESM1, with supporting documentation, occurred

in June 2010 (see www.cesm.ucar.edu/models/cesm1.0/). A large number of simulations with it have been conducted, all of which are available for community analysis. They include simulations submitted to phase 5 of the Coupled Model Inter-comparison Project (CMIP5; Taylor et al. 2012). As such, CESM will make a major contribution to the next U.S. National Assessment of Climate Change, as well as the Fifth Assessment Report (AR5) of the IPCC.

This article outlines some of the general simulation features and capabilities of CESM1, emphasizing extensions beyond the capabilities of CCSM4, and it highlights an ambitious set of CESM1 climate change simulations available for community analysis. It also briefly describes plans for future development of this new modeling system.

OVERVIEW OF MAJOR COMPONENTS AND NEW EARTH SYSTEM CAPABILITIES.

CESM1 consists of component models with many new capabilities that can be coupled in different configurations (Fig. 1). In all cases, geophysical fluxes across the components are exchanged via a central coupler (Craig et al. 2012). While CESM1 supersedes CCSM4, users can run equivalent CCSM4 experiments from the CESM1 code base by using the CCSM4 component set (Gent et al. 2011). Alternatively, the atmospheric component of CESM1 can be the latest version of the Community Atmosphere Model [version 5 (CAM5)], the high-top atmosphere (WACCM), or CAM with chemistry (CAM-CHEM). In these cases, the model configurations are referred to as CESM1(CAM5), CESM1(WACCM), and CESM1(CHEM), respectively. Likewise, CESM1(BGC) refers to a configuration with active biogeochemistry and a prognostic carbon cycle with nitrogen limitation, while CESM1(CISM) refers to a configuration with an active Greenland Ice Sheet



FIG. 1. Schematic of the different component models in CESM1.

using the Glimmer Community Ice Sheet Model (Glimmer-CISM). Many other configurations are possible, but those mentioned above are the primary scientifically validated ones for which climate simulations have been completed and are available for community analysis (Table 1). These component models and the new capabilities associated with them are thus the focus of this article, and they are described briefly below.

Atmosphere. Two different versions of the CAM are available with CESM1. The seventh generation of atmospheric models used for the CCSM/CESM activity is CAM, version 4 (CAM4; Neale et al. 2013), and it is the atmospheric component of CCSM4. Many CAM4 simulation characteristics are discussed in the aforementioned *Journal of Climate* special collection. In this article, we focus on CAM5, the eighth-generation atmospheric general

TABLE 1. Supported configurations of CESM1 and relevant CMIP5 simulations. For the PI control run, the number of years available is listed. For the twentieth- and twenty-first-century integrations, the number of ensemble members is shown. Twentieth-century runs are from 1850 to 2005, while the RCP simulations cover 2005–2100. One ensemble member for each RCP for both CCSM4 and CESM1(CAM5) extends to 2300. For CESM1(WACCM) three of the four twentieth-century ensemble members only cover 1955–2005, while two of the three RCP 4.5 simulations stop in 2065. Output from all of these simulations is available from the CMIP5 archive except for the CESM1(CISM) simulations.

Model configuration	Active component models	PI control (yr)	Twentieth century	RCP 2.6	RCP 4.5	RCP 6.0	RCP 8.5
CCSM4	CAM4 CLM4 CICE4 POP2	500	6	6	6	6	6
CESM1(CAM5)	CAM5 CLM4 CICE4 POP2	319	3	3	3	3	3
CESM1(CHEM)	CAM-CHEM CLM4 CICE4 POP2	222	3	0	0	0	0
CESM1(WACCM)	WACCM4 CLM4 CICE4 POP2	200	4	0	3	0	1
CESM1(BGC) (prescribed concentrations)	CAM4 CLM4 CICE4 POP2	500	1	0	1	0	1
CESM1(BGC) (prescribed emissions)	CAM4 CLM4 CICE4 POP2	500	1	0	0	0	1
CESM1(CISM)	CAM4 CLM4 CICE4 POP2 CISM	100	1	0	0	0	1

circulation model released with CESM1. This model is a significant advancement from CAM4. While treatment of the atmospheric dynamics is very similar to CAM4, parameterizations of diabatic processes (with the exception of the deep convection parameterization) differ substantially. Internal consistency across process representation was especially emphasized during the development of CAM5, and the new parameterizations reflect either an improved understanding of the process itself or the way it should be represented for climate applications. Considerable emphasis was placed on improvements to the treatment of water substances (liquid, ice, vapor) and aerosols, and their interactions with the rest of the climate system. New parameterizations were developed for cloud fraction, cloud particle formation, aerosol formation and removal, radiative properties of the aerosols and cloud particles, radiative transfer, and convection and turbulence. The new parameterizations allow aerosol indirect effects to be estimated with CAM5, which was not possible in CAM4, and they also affect many other aspects of the model simulation.

The treatment for stratiform cloud formation, condensation, and evaporation (macrophysics) is described in Neale et al. (2012). A two-moment microphysical parameterization (Morrison and Gettelman 2008; Gettelman et al. 2008) is used to predict the mass and number of smaller cloud particles (liquid and ice), while the mass and number of larger precipitating particles (rain and snow) are diagnosed. Cloud microphysics is coupled to a modal aerosol treatment (Liu et al. 2012; Ghan et al. 2012) that predicts the aerosol mass and number of internal mixtures of black and organic carbon, dust, sea salt, and sulfate aerosols. A two-stream correlated- k distribution Rapid Radiative Transfer Model for GCMs (RRTMG; Iacono et al. 2008) is used to calculate the radiative fluxes and heating rates for gaseous and condensed atmospheric species. A statistical technique is used to represent subgrid-scale cloud overlap (Pincus and Morcrette 2003). New moist turbulence (Bretherton and Park 2009) and shallow convection parameterization schemes (Park and Bretherton 2009) provide substantial improvements to the simulation of shallow clouds in the boundary layer.

Atmospheric chemistry. CAM-CHEM represents the implementation of atmospheric chemistry in CESM. The atmospheric chemistry can be enabled with computed or specified (e.g., from an atmospheric analysis or reanalysis product) meteorological fields. In either case, the chemistry is fully integrated into

CAM4 (Lamarque et al. 2012) and CAM5, and the representation of dynamics (including transport) and physics (radiation, convection, and large-scale precipitation; boundary layer and diffusion) is the same as in the standard CAM. All subroutines responsible for the representation of chemistry are included in the build of CESM only when explicitly requested; therefore, users are not impacted by the additional code and cost to simulate chemistry if they are only interested in a climate simulation for which the atmospheric composition is specified.

Chemically active constituents can affect climate through radiation (gas and aerosols), nitrogen deposition (impact on carbon–nitrogen cycling in the land and ocean model biogeochemistry components), aerosol deposition (black carbon and dust on snow and ice), and cloud–aerosol interactions (in the case of CAM5 only). CAM-CHEM is flexible in handling various representations of chemistry that differ in the number of chemical species and chemical reactions. In this way, users can configure the model with the chemistry best adapted to their specific problem.

High-top atmosphere. The WACCM is a configuration of the atmospheric component of CESM in which the atmosphere has a vertical domain that spans from the surface to the lower thermosphere (~140 km). As in CAM-CHEM, WACCM includes interactive chemistry that is fully integrated into CAM dynamics and physics. The method by which chemistry is solved is identical, so that CAM-CHEM and WACCM differ only in terms of the number of species and chemical reactions. WACCM typically uses a scheme that is more tailored to the middle and upper atmosphere while being computationally cheaper in the troposphere than CAM-CHEM. The scheme includes heterogeneous chemistry that can lead to the development of the ozone hole and ion chemistry necessary to simulate the ionosphere.

The underlying physics in WACCM is the same as in CAM4 (Neale et al. 2013), with the addition of processes essential for reproducing the observed mean meridional circulation in the stratosphere and mesosphere and the distribution of minor constituents. These include the parameterization of nonorographic gravity waves (i.e., those generated from deep convection and fronts), molecular diffusion, energetic particle precipitation, and nonlocal thermodynamic equilibrium radiative transfer. A quasi-biennial oscillation in the winds of the tropical stratosphere is imposed by relaxing the zonal wind between 86 and 4 hPa to the observed interannual variability (Marsh et al. 2013).

WACCM has been extensively compared to observations and other chemistry–climate models. It has been found to perform well in the model evaluation exercise conducted by the Stratospheric Processes and their Role in Climate (SPARC) project of the World Climate Research Programme (WCRP; see SPARC CCMVal 2010). Fully resolving the stratosphere leads to improvements in the representation of atmospheric dynamical variability. In particular, breakdowns of the Northern Hemisphere wintertime vortex, known as major stratospheric sudden warmings, occur with a frequency that is close to observed, while in CCSM4 they are almost entirely absent (Marsh et al. 2013).

Land. The Community Land Model (CLM) is designed to represent and enable study of the physical, chemical, and biological processes by which terrestrial ecosystems affect and are affected by climate across a variety of spatial and temporal scales. The central theme is that terrestrial ecosystems, through their cycling of energy, water, chemical elements, and trace gases, are important determinants of climate. The land surface is a critical interface through which climate change impacts humans and ecosystems and through which humans and ecosystems can effect global environmental change.

The CLM4 (Lawrence et al. 2011; Oleson et al. 2010) is used in both CESM1 and CCSM4. New features relative to previous versions of CLM include a prognostic carbon–nitrogen (CN) model (Thornton et al. 2007), an urban canyon model (Oleson et al. 2008), and a transient land cover and land use change capability, including wood harvest (Lawrence et al. 2012a). A revised snow model incorporates the Snow, Ice, and Aerosol Radiation (SNICAR) model (Flanner et al. 2007). SNICAR includes aerosol deposition of black carbon and dust (either prescribed or determined prognostically by CAM), grain-size dependent snow aging, and vertically resolved snowpack heating. Dust is mobilized from the land by wind (Zender et al. 2003) and passed to the atmospheric aerosol model. The representation of permafrost is significantly improved in CLM4 (Lawrence et al. 2012b). The dynamic global vegetation model in CLM3 is merged with CN in CLM4 (Castillo et al. 2012), although it is not active for either the CCSM4 or the CESM1 CMIP5 simulations described here. Finally, CLM4 possesses an interactive crop management model (Levis et al. 2012) and an irrigation scheme (Sacks et al. 2009). The crop model is based on agricultural version of the Integrated Biosphere Simulator (Agro-IBIS; Kucharik and Brye 2003) and includes parameters

for corn, soybean, and temperate cereals. When irrigation is enabled, the cropland area of each grid cell is divided into an irrigated and unirrigated fraction according to a dataset of areas equipped for irrigation. Biogenic volatile organic compound emissions from vegetation are also calculated and passed to CAM-CHEM.

Sea ice. The sea ice component of CESM1 utilizes version 4 of the Los Alamos National Laboratory (LANL) Community Ice Code (CICE4; Hunke and Lipscomb 2008) with some additions. It includes the thermodynamics of Bitz and Lipscomb (1999), the elastic–viscous–plastic dynamics of Hunke and Dukowicz (2002), and a subgrid-scale representation of ice thickness distribution following Thorndike et al. (1975) and Rothrock (1975). As documented in Holland et al. (2012), the most notable improvements in the sea ice component of CESM1 compared to earlier model versions includes a multiple-scattering shortwave radiation treatment (Briegleb and Light 2007) and associated capabilities to simulate explicitly melt pond evolution and the deposition and cycling of aerosols (dust and black carbon) within the ice pack. These new capabilities influence both the mean climate state and simulated climate feedbacks at high latitudes (Holland et al. 2012).

Ocean. CESM1, like CCSM4, utilizes the LANL Parallel Ocean Program, version 2 (POP2; Smith et al. 2010), as the ocean model component. This is a level coordinate primitive equation model that, in the standard configuration, uses 60 levels in the vertical varying from 10 m near the surface to 250 m at depth. Compared to previous model versions, several notable enhancements are incorporated. Climate Variability and Predictability (CLIVAR) Climate Process Teams (<http://www2.cgd.ucar.edu/research/clivar-climate-process-teams>) produced parameterizations to mimic the Denmark Strait, Faroe Bank Channel, Ross Sea, and Weddell Sea overflows (Danabasoglu et al. 2010; Briegleb et al. 2010); to account for submesoscale eddy effects in the mixed layer (Fox-Kemper et al. 2008); and to improve the representation of mesoscale eddies in the ocean mixed layer, in the nearly adiabatic deep ocean, as well as through the transition region in between (Danabasoglu et al. 2008). Other improvements include modifications and general reductions to the horizontal viscosity (Jochum et al. 2008) and an abyssal tidal mixing parameterization (Jayne 2009). More discussion of the ocean model physics and simulations is available in Danabasoglu et al. (2012).

Biogeochemistry. The CESM1 has the capability to include a fully prognostic carbon cycle (Lindsay et al. 2013, manuscript submitted to *J. Climate*). The land carbon model is coupled to the biogeophysics and hydrology in the model, and it simulates photosynthesis, respiration, litter, and soil carbon and leaf phenology. The model includes colimitation by nitrogen and nitrogen cycling through the soil, litter, roots and vegetation (Lindsay et al. 2013, manuscript submitted to *J. Climate*; Thornton et al. 2009, 2007). Vegetation is composed of leaves, coarse and fine roots and stems, and carbon storage pools. Four organic carbon and nitrogen pools exist in the soils, interacting with the vegetation, roots, coarse woody debris, and mineral pools. Deposition of nitrogen to the soils (based on Lamarque et al. 2010) adds to the available nitrogen. A prognostic fire model simulates wildfire (Thonicke et al. 2001). Transitions in vegetation distribution are prescribed through a land cover change dataset (Hurtt et al. 2006; Lawrence et al. 2012). Dynamic vegetation biogeography is turned off for all CMIP5 simulations because CLM4 cannot yet run with prescribed land cover change and dynamic vegetation simultaneously. This is a structural software limitation of the model that will be rectified in future versions.

The ocean carbon model is based on the nutrient–phytoplankton–zooplankton–detritus approach (Moore et al. 2004). The model predicts nutrient distributions (N, Si, Fe, P), light availability, and temperature in each of the vertical layers of the model, which controls three phytoplankton functional types: diatoms, picophytoplankton/nanophytoplankton, and diazotrophs (nitrogen-fixing organisms). The ocean chemistry allows full carbonate chemistry. Sources of nutrients include atmospheric deposition (nitrogen and dust, as calculated interactively in CAM-CHEM or from input datasets) and sedimentary sources. Sinking particles can be associated with ballast, and the presence of ballast changes the remineralization length scale assumed for the model.

Land ice. It has been assumed in most global climate models that ice sheets are fixed in elevation and extent. Recent observations, however, have shown that ice sheets can respond to changing ocean and atmospheric forcing on annual to decadal time scales. Mass loss from the Greenland and Antarctic Ice Sheets is accelerating and is expected to make a significant contribution to twenty-first-century sea level rise (e.g., Allison et al. 2009; Rignot et al. 2011). As a first step toward simulating these changes, CESM1 includes a dynamic ice sheet component,

Glimmer-CISM (Rutt et al. 2009). Glimmer-CISM is a thermomechanical ice sheet model that solves three-dimensional equations for conservation of momentum, mass, and internal energy, with simple parameterizations of basal sliding and iceberg calving. Glimmer-CISM 1.6, the version in CESM1, uses the shallow-ice approximation, which is valid for slow flow dominated by vertical shear. More sophisticated higher-order models (e.g., Pattyn et al. 2008; Price et al. 2011), which are needed to simulate fast flow in ice shelves, ice streams, and outlet glaciers, will be included in future CESM releases.

The interface of Glimmer-CISM enables flexible coupling to climate models. CESM1 currently supports coupling to a dynamic Greenland Ice Sheet (GrIS), which is simulated on a 5-km rectangular mesh. The ice sheet surface mass balance (SMB) and surface temperature are computed in the land model, CLM, in multiple elevation classes in the glaciated part of each grid cell. The SMB is positive when the snow depth exceeds the maximum allowed value and additional snow turns to ice, and the SMB is negative when the snow depth is zero and the underlying ice melts. This approach is more physically based than the positive-degree-day schemes often used to force ice sheet models (Bougamont et al. 2007) and ensures that ice sheet mass changes are consistent with CLM's surface energy budget. The resulting SMB and surface temperature in each elevation class are passed to Glimmer-CISM via the coupler and downscaled to the ice sheet mesh. Lipscomb et al. (2013) describe the model implementation in detail. Initial work has focused on simulating and validating the SMB of the GrIS, as described later.

Infrastructure and model performance. Novel infrastructure capabilities in CESM1 permit new flexibility and extensibility to address the challenges involved in Earth system modeling. An integral part of CESM1 is the implementation of a coupling architecture that provides the ability to use a single code base in a start-to-end development cycle—from model parameterization development (that might only require a single processor) to ultra-high resolution simulations on high-performance computing (HPC) platforms using tens of thousands of cores. CESM1 has the flexibility of running model components sequentially, concurrently, or in a mixed sequential/concurrent mode, and results of a given simulation are independent of the component processor layouts chosen. The CESM1 coupling architecture also provides “plug and play” capability of data and active components and includes a user-friendly scripting

system and informative timing utilities. Together, these tools enable a user to create a wide variety of “out of the box” experiments for different model configurations and resolutions and also to determine the optimal load balance for those experiments to ensure maximal throughput and efficiency. Further information on the CESM coupling infrastructure is available in Craig et al. (2012).

CMIP5 SIMULATION OVERVIEW. There are a large number of CCSM4 simulations that have contributed to the CMIP5 (Taylor et al. 2012). These include a long preindustrial (PI) control simulation and multiple twenty- and twenty-first-century ensemble members, all described in detail in the *Journal of Climate* special collection. There are also a number of initialized “decadal prediction” experiments (e.g., Yeager et al. 2012).

Long-term climate simulations for a PI state, twentieth-century historical climate, and twenty-first-century projections have also been performed for various CESM1 configurations. These, along with the length of the PI simulations and the number and length of twentieth- and twenty-first-century ensemble members, are listed in Table 1. All of these simulations, except for the CESM1(CISM) runs, are available to the community for analysis through the CMIP5 archive maintained by the Program for Climate Model Diagnosis and Intercomparison (PCMDI) at the Lawrence Livermore National Laboratory.

For simulations from 1850 through 2005, physical climate simulations utilize observationally based external forcing estimates (e.g., time-varying greenhouse gas concentrations, volcanic aerosols, and solar variability; see Lamarque et al. 2010). Different representative concentration pathways (RCPs) from integrated assessment models are used for twenty-first-century simulations (e.g., van Vuuren et al. 2007). In contrast to physical climate simulations, the standard CESM1(BGC) simulations were forced with carbon dioxide emissions (instead of concentrations) and carbon dioxide concentrations were predicted in the model.

In all supported configurations listed in Table 1, the ocean and sea ice components use a nominal 1° horizontal resolution, with 60 vertical levels in the ocean. The meridional resolution is $\sim 1/3^\circ$ near the equator, and in the Northern Hemisphere the pole is displaced into Greenland to avoid merging meridians near the North Pole. In the atmosphere and land components, all configurations have a horizontal resolution of about 1°, with 30 layers in the atmosphere. The exception is

CESM1(WACCM), which uses an atmospheric horizontal resolution of approximately 2° with 66 vertical levels extending from the surface to 5.1×10^{-6} hPa.

In tuning the physical climate configurations of CESM1, the component models were finalized independently through stand-alone integrations with observed boundary forcing. These included simulations of the various atmospheric components forced with observed sea surface temperatures, and ocean, sea ice, and land component simulations forced by observed atmospheric conditions. Once these components were coupled, tuning was performed on PI and twentieth-century climate simulations with modifications allowed only to 1) sea ice albedos, within observational uncertainties, in order to obtain a reasonable mean Arctic sea ice thickness; and 2) cloud parameters, in order to obtain radiation balance at the top of the atmosphere. Gent et al. (2011) provide additional details on the tuning procedures. For CESM1(BGC) integrations, ocean biogeochemical tracers were spun up in a 1,000-yr ocean-only integration forced with a 5-yr repeating cycle of high-frequency CCSM4 atmospheric surface forcing. To avoid drift in the ocean physical solution, the ocean physical state was reset to conditions from the CCSM4 coupled run at the end of every 5-yr forcing cycle. The initial conditions for the land biogeochemistry component were also taken from the same time in the fully coupled run.

RESULTS FROM CESM1 CONFIGURATIONS. In addition to the CCSM4 special collection of papers, there is also a *Journal of Climate* collection in preparation documenting CESM1 and its simulation characteristics. In this article, we show a limited number of simulation results that are intended to highlight new scientific results that are possible with the enhanced capabilities available to the community for research employing CESM1.

CESM1(CAM5). The model advancements incorporated into CAM5 result in considerable changes in feedback strengths for the globe (Gettelman et al. 2012). The equilibrium climate sensitivity of CESM1(CAM5) is 4.1°C (Gettelman et al. 2012) compared to 3.2°C in the standard version of CCSM4 (Bitz et al. 2012), while the transient climate sensitivity of CESM1(CAM5) is 2.3°C compared to 1.7°C for CCSM4. The differences are mostly due to more positive cloud feedbacks, especially in the tropical trade cumulus regime and the midlatitude storm tracks (Gettelman et al. 2012), and higher CO₂ radiative forcing in CAM5 (Kay et al. 2012b). Several

parameterizations contribute to changes in tropical cloud feedbacks between CAM4 and CAM5, but a new shallow convection scheme causes the largest midlatitude feedback differences and the largest change in climate sensitivity (Gettelman et al. 2012).

The inclusion of an aerosol indirect effect leads to large changes in both the twentieth- and twenty-first-century transient climate response in CESM1(CAM5) relative to CCSM4 (Fig. 2). Since CCSM4 does not include an aerosol indirect effect, its total aerosol cooling is much weaker. Ghan et al. (2012) estimate the anthropogenic aerosol forcing in CAM5 to be -1.5 W m^{-2} (-2 W m^{-2} shortwave + 0.5 W m^{-2} longwave). Over the twentieth century, this negative forcing produces more realistic warming than in CCSM4, which overestimates the twentieth-century warming relative to observations (Gent et al. 2011;

Meehl et al. 2012). The reduced warming is not uniform across the globe but instead is largest in the Arctic (Fig. 2, middle left) as a result of sea-ice-related feedbacks. In contrast, the twenty-first-century warming under RCP 8.5 is considerably larger in CESM1(CAM5), with much of the Arctic experiencing over 3°C more warming compared to CCSM4 (Fig. 2, middle right). The larger future Arctic warming in CESM1(CAM5) is consistent with feedback analysis showing less negative shortwave cloud feedbacks and more positive surface albedo feedbacks compared to CAM4 (Kay et al. 2012b).

A robust match between observed and modeled cloud properties is an important metric of modeled cloud processes. Satellite observations and model-data analyses that simulate the corresponding instruments are powerful tools to evaluate cloud biases in models.

Despite having similar global mean and spatial patterns of cloud radiative forcing (not shown), CAM5 has more realistic clouds than CAM4 (Kay et al. 2012a). In particular, CAM5 exhibits substantial improvement in three long-standing cloud biases (Zhang et al. 2005). Those are the underestimation

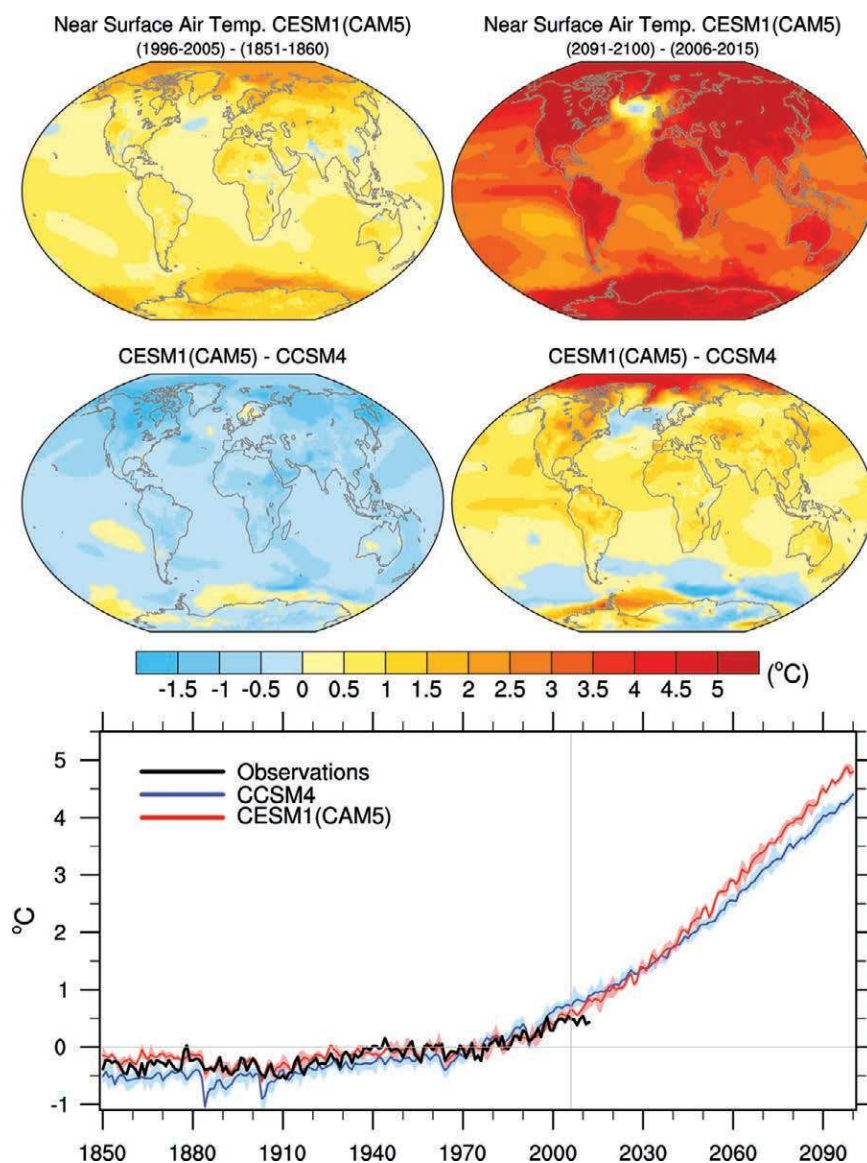


FIG. 2. Decadal-mean, ensemble-average difference in near-surface air temperature ($^\circ\text{C}$) (top left) from PI to present day and (top right) over the twenty-first century (for RCP 8.5) simulated by CESM1(CAM5). (middle) Over the same periods, the differences from simulations with CCSM4, where the blue (yellow/red) colors indicate the temperature increase in CESM1(CAM5) is smaller (larger). (bottom) Time series of the annually and globally averaged near-surface air temperature for each model from 1850 to 2100. Shaded regions show the spread in three ensemble members from CESM1(CAM5) and six ensemble members from CCSM4. Observations (1850–2005) are from Morice et al. (2012).

of total cloud, the overestimation of optically thick cloud, and the underestimation of midlevel cloud. Comparisons of observed and cloud-simulator-diagnosed global column-integrated cloud optical depth distributions (Fig. 3) illustrate that CAM5 is much closer to independent observational estimates than CAM4. Moreover, this is the result of new and improved model physics, not tuning.

One of the most pronounced improvements following CCSM3 (Collins et al. 2006) was the simulation of variability associated with the El Niño–Southern Oscillation (ENSO) phenomenon (Gent et al. 2011), including a lengthened and more realistic 3–6-yr period, a larger range of amplitude and frequency of events, and the longer duration of La Niña compared to El Niño (Deser et al. 2012). These remain in CESM1(CAM5) simulations (not shown). An additional and notable improvement in CAM5 is the simulation of atmospheric high pressure blocking. This is primarily due to an additional parameterization of surface stress in CAM5 meant to represent the turbulent drag on the resolved flow by subgrid-scale topographic variations, which has a significant impact on reducing mean midlatitude low surface pressure

biases in the storm-track regions in both uncoupled (e.g., prescribed sea surface temperature) and coupled simulations (not shown). The blocking frequency (D’Andrea et al. 1998) for boreal spring in the Atlantic–Eurasian sector shows a significant underestimation in CAM4 relative to observations, with a shift in the maximum too far into Russia (Fig. 4). The blocking frequency in CAM5 simulations, on the other hand, is much closer to observations, although problems still persist such as the underestimate over the western Atlantic. Increasing the horizontal resolution of CAM5 does not result in a systematic improvement over the 1° results (see also Scaife et al. 2010), although it better captures the double maxima of Atlantic and European blocking (Fig. 4).

Many aspects of the Arctic simulation are improved in CESM1(CAM5), including clouds (Kay et al. 2012a), permafrost distribution and temperature (Lawrence et al. 2012b; Meehl et al. 2013), and sea ice. The simulation of Arctic sea ice by CESM1(CAM5) is illustrated in Fig. 5. The simulated annual cycle of late-twentieth-century sea ice extent compares very well to observations (Fig. 5a), as monthly-mean climatological values are generally within one standard deviation

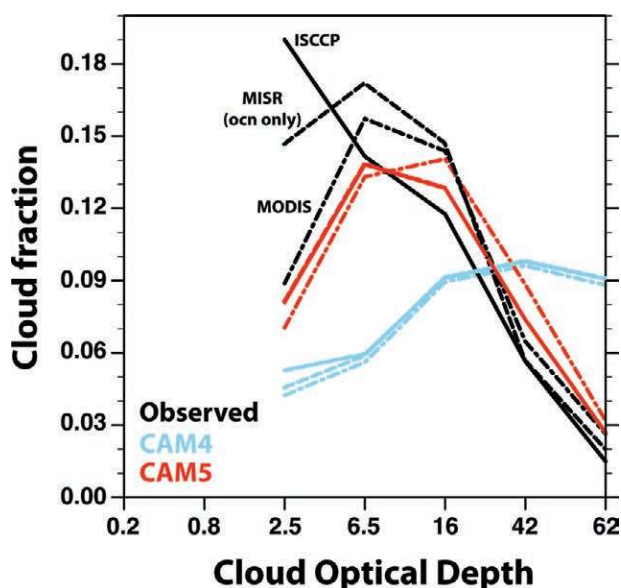


FIG. 3. Global column-integrated cloud optical depth distributions from three satellite observations and their corresponding CAM4 and CAM5 outputs from instrument simulators (Bodas-Salcedo et al. 2011). Comparisons use International Satellite Cloud Climatology Project (ISCCP), the Multiangle Imaging Spectroradiometer (MISR), and the Moderate Resolution Imaging Spectroradiometer (MODIS) observations. (Adapted from Kay et al. 2012a.)

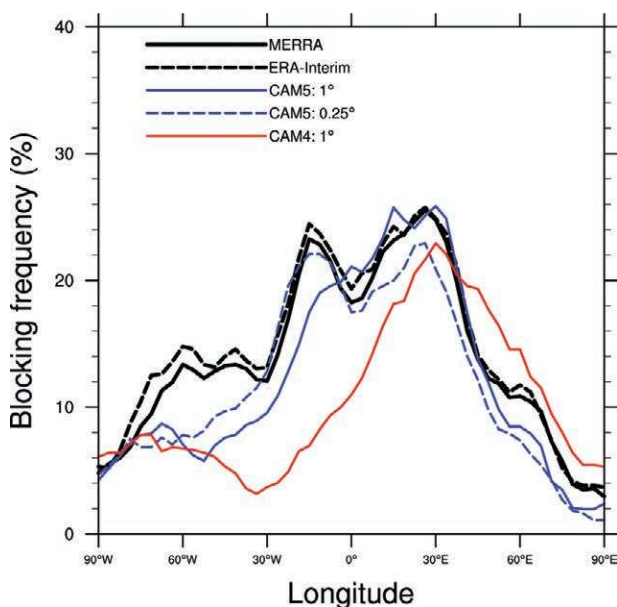


FIG. 4. The frequency of atmospheric blocking events over the Atlantic and Eurasian sectors during boreal spring (Mar–May) over the decade 1990–99. Observational estimates (black curves) are from two atmospheric reanalysis datasets [Modern-Era Retrospective analysis for Research and Applications (MERRA) and European Centre for Medium-Range Weather Forecasts (ERA-Interim)], while the blocking frequency from uncoupled (prescribed sea surface temperature) simulations with CAM5 (CAM4) is in blue (red).

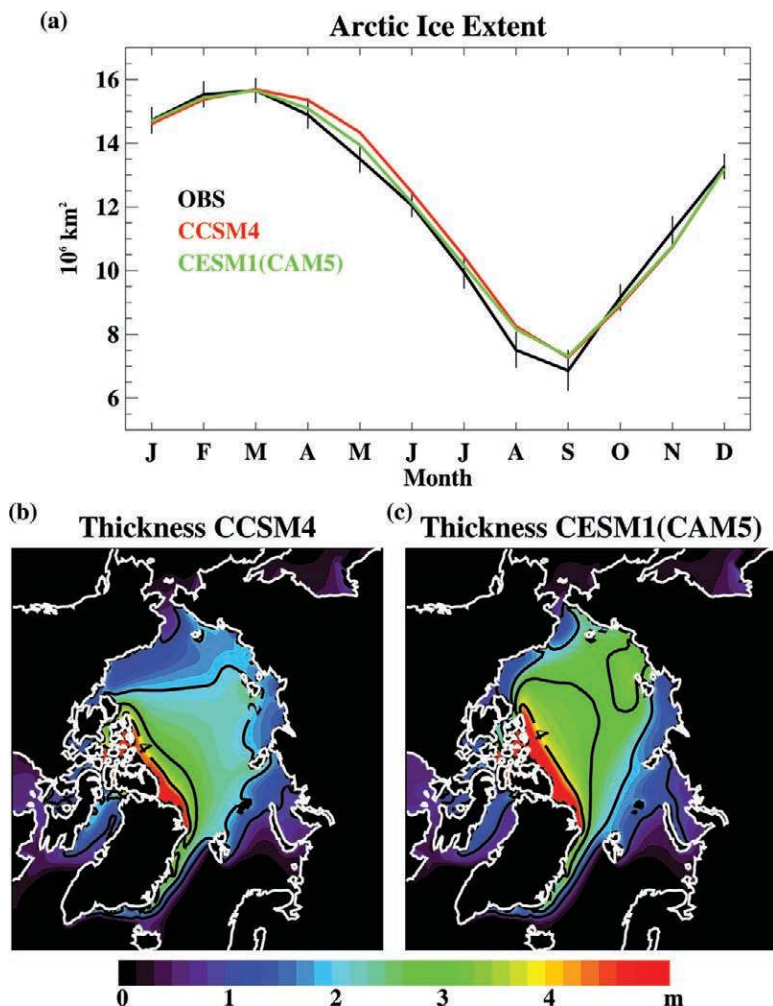


FIG. 5. (a) Monthly-mean values of Northern Hemisphere ice extent, defined as the total area with larger than 15% ice concentration, for the observations (black), CCSM4 (red), and CESM1 (CAM5) (green). Black vertical lines indicate the observational standard deviation. (b) Annual mean ice thickness in CCSM4 and (c) CESM1(CAM5). Black lines are 1-m contours. Means are calculated for 1979–2005.

of the satellite-derived observations (Fetterer et al. 2002). This is similar to the CCSM4 results, which also exhibit a well-simulated seasonal progression of the sea ice edge (Jahn et al. 2012). While minimal albedo tuning is done to achieve a reasonable mean thickness, this tuning has a limited effect on the spatial distribution of ice within the Arctic, which depends critically on wind forcing and relative heating across the basin. As shown in Figs. 5b and 5c, this distribution is in good agreement with observed conditions (e.g., Bourke and Garrett 1987; Kwok and Cunningham 2008). In particular, the thickest ice is present north of Greenland and the Canadian Arctic Archipelago, and the ice thins across the basin toward the Siberian coast. Compared to CCSM4, the CESM1(CAM5) ice is generally thicker, which may be a consequence of the reduced

twentieth-century warming (Fig. 2). Both CCSM4 and CESM1(CAM5) exhibit late-twentieth-century sea ice loss that is consistent with observations (Vavrus et al. 2012; Kay et al. 2011; Stroeve et al. 2012).

CESM1(CHEM). The inclusion of atmospheric chemistry within CAM allows for the determination of changing atmospheric composition given assumptions about future emissions. Results from the CAM-CHEM simulations (Lamarque et al. 2010, 2011) have been used to define, for both CCSM4 and CESM1 CMIP5 simulations, the time-varying concentrations of short-lived greenhouse gases, aerosols, oxidant fields (for CESM1) and deposition fields of nitrogen, dust, and black carbon. The CAM-CHEM simulations include a representation of tropospheric and stratospheric chemistry, and a specific configuration was chosen to provide a continuous (in time and space) distribution across the tropopause, where the sensitivity of the radiative forcing to changes in ozone is largest (Lacis and Hansen 1974; Worden et al. 2008).

Changes in atmospheric composition arise from changes in emissions and changes in the rates of production and removal of the specific compound of interest. In terms of tropospheric ozone (Lamarque et al. 2011), CESM1(CHEM) simulates a gradual increase until 1950, with a strong rise through 2000 (not shown) associated with increasing emissions of ozone precursors, in particular nitrogen oxides (Lamarque et al. 2010). Regional increases in nitrogen oxide emissions are the main drivers of regional changes in nitrogen deposition (Fig. 6). After 2000, the various RCPs provide different emission pathways, although they tend to provide similar decreasing emissions for ozone precursors by the late twenty-first century. This leads to very similar estimates of future changes in nitrogen deposition across the RCPs (Fig. 6), except for the deposition associated with ammonia emissions. These are projected to increase in all RCPs but RCP 4.5. For tropospheric ozone, the main outlier is RCP 8.5, which is influenced by both a very large increase

in future methane concentrations (Riahi et al. 2011) and increases in stratospheric ozone (Lamarque et al. 2011). Stratospheric ozone contributes to tropospheric ozone mostly through extratropical transport. Future stratospheric ozone levels are projected to increase as a result of the projected disappearance of man-made halogen compounds and because of decreases in stratospheric temperatures, lowering gas-phase ozone loss rates (Kawase et al. 2011). CESM1(CHEM), through its representation of atmospheric chemistry, is able to simulate the combination of these factors that lead to a strong differentiation among the various RCPs in tropospheric ozone levels by 2100.

CESM(WACCM). Changing atmospheric composition has the potential to modify atmospheric conditions well above the troposphere. With the inclusion of WACCM in CESM, these effects and their potential implications for surface climate can be investigated and quantified. CESM1(WACCM) simulations show very large changes in the stratosphere and mesosphere from the preindustrial era to the end of the twenty-first century (Marsh et al. 2013). The development of the stratospheric ozone hole in the model agrees

with observations (not shown). In particular, the minimum column ozone approaches 100 Dobson units in the late 1990s. Ozone loss and increasing greenhouse gas concentrations led to a cooling of the polar cap in the lower stratosphere of -4.6 ± 3.2 K decade⁻¹ over the period 1979–2003 (Calvo et al. 2012), which is comparable to the observed trend of -3.75 K decade⁻¹ reported by Thompson and Solomon (2005). Associated with this cooling is a 10 m s^{-1} increase, centered near 65°S at 30 hPa, in the zonal-mean zonal wind during austral summer (Fig. 7). These changes are partially reversed over 2005–50, with a weakening of the summertime winds due to the projected decrease in man-made halogens and consequent recovery of the ozone layer.

Stratospheric changes are not restricted to polar regions. Looking into the future, CESM1(WACCM) projects global mean upper-stratospheric temperature will drop from the present-day value by 6 K (15 K) under RCP 4.5 (8.5) by 2100 (Eyring et al. 2013). This cooling, along with a decrease in halogens, will lead to a “super recovery” of stratospheric ozone in which the ozone column at some latitudes will exceed preozone hole (~1980) values.

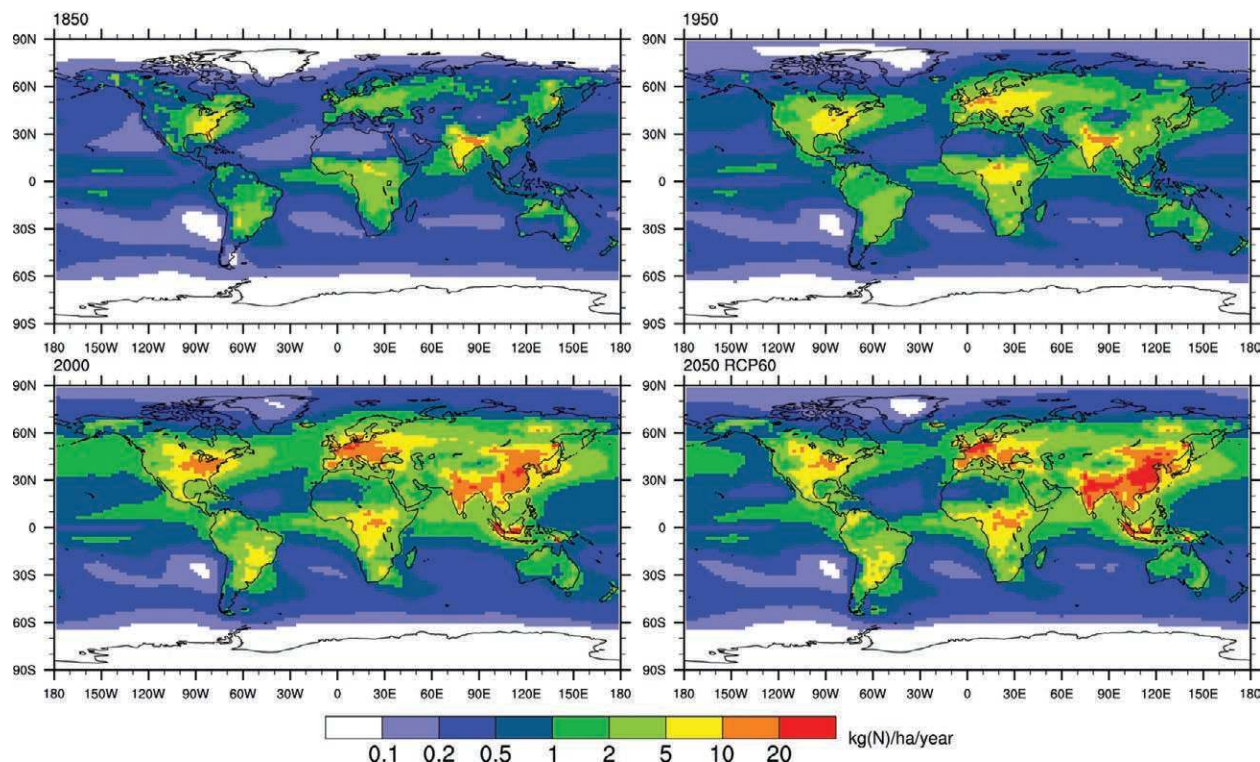


FIG. 6. Time evolution of nitrogen deposition ($\text{kg ha}^{-1} \text{ yr}^{-1}$) computed from CAM-CHEM simulations (Lamarque et al. 2010, 2011) and used as input into the land and ocean biogeochemistry components. Deposition is shown for (top left) 1850, (top right) 1950, (bottom left) 2000, and (bottom right) 2050. The last is from RCP 6.0 only, since all the RCPs display a very similar global distribution of N deposition, with differences over China being the main exception.

CESM1(BGC). For the first time in the history of the project, the release version of CESM1 includes a coupled carbon–climate model. This model includes nutrient cycling on land and oceans and the colimitation of land biogeochemistry by nitrogen (N). Historical (1850–2005) simulations (Lindsay et al. 2013, manuscript submitted to *J. Climate*) suggest the model is able to capture the observed CO₂ increase up to approximately 1950 (Fig. 8a). However, after 1950, the model simulations show more CO₂ in the atmosphere than observed. This is because the modeled uptake of anthropogenic CO₂ is lower than observational estimates (Fig. 8b). Analysis of the simulated ocean and land carbon pools suggests that both the land and ocean models underestimate uptake compared to model/observational syntheses (e.g., Canadell et al. 2007) (Figs. 8c and 8d).

A prognostic carbon cycle permits CESM1(BGC) to predict the evolution of natural carbon sinks and, thus, atmospheric CO₂ as a function of specified emissions for future projections (Fig. 9a; Long et al. 2013, manuscript submitted to *J. Climate*). Furthermore, the model provides a framework in which to evaluate the sensitivity of carbon sinks to climate change and other factors such as N deposition (Figs. 9b and 9c). Carbon–climate feedbacks reduce carbon absorption by both the land and ocean (e.g., Friedlingstein and Prentice 2010). The terrestrial carbon sink is also sensitive to N colimitation (e.g., Thornton et al. 2009), which can reduce the

effectiveness of this sink, while the ocean carbon sink does not display significant sensitivity to changing N deposition (Figs. 9b and 9c). Inclusion of the carbon cycle in CESM1(BGC) provides valuable and more complete information on the possible response of the land and ocean to changes in climate.

CESM1(CISM). Simulations with an interactive Greenland Ice Sheet (GrIS) have been completed for a preindustrial, twentieth-century, and twenty-first-century RCP 8.5 scenario (Vizcaíno et al. 2013a,b, manuscript submitted to *J. Climate*). The mean surface mass balance for the GrIS during the latter part of the twentieth-century run (1960–2005) is shown in Fig. 10a. The SMB generally agrees well with results from the Regional Atmospheric Climate Model, version 2 (RACMO2; van Angelen et al. 2012) for the same period (Fig. 10b), which is taken as an estimate of the observed SMB. The total SMB for the GrIS in the CESM1(CISM) simulation is $359 \pm 120 \text{ Gt yr}^{-1}$, compared to $376 \pm 117 \text{ Gt yr}^{-1}$ from RACMO2, where the ranges denote one standard deviation. CESM1(CISM) underestimates accumulation in southeast Greenland and overestimates accumulation in the interior, probably because of the coarser resolution and smoother orography. However, CESM1(CISM) successfully captures the ablation zones along the north, northeast, and west margins of the ice sheet, as well as local snowfall maxima along the west coast.

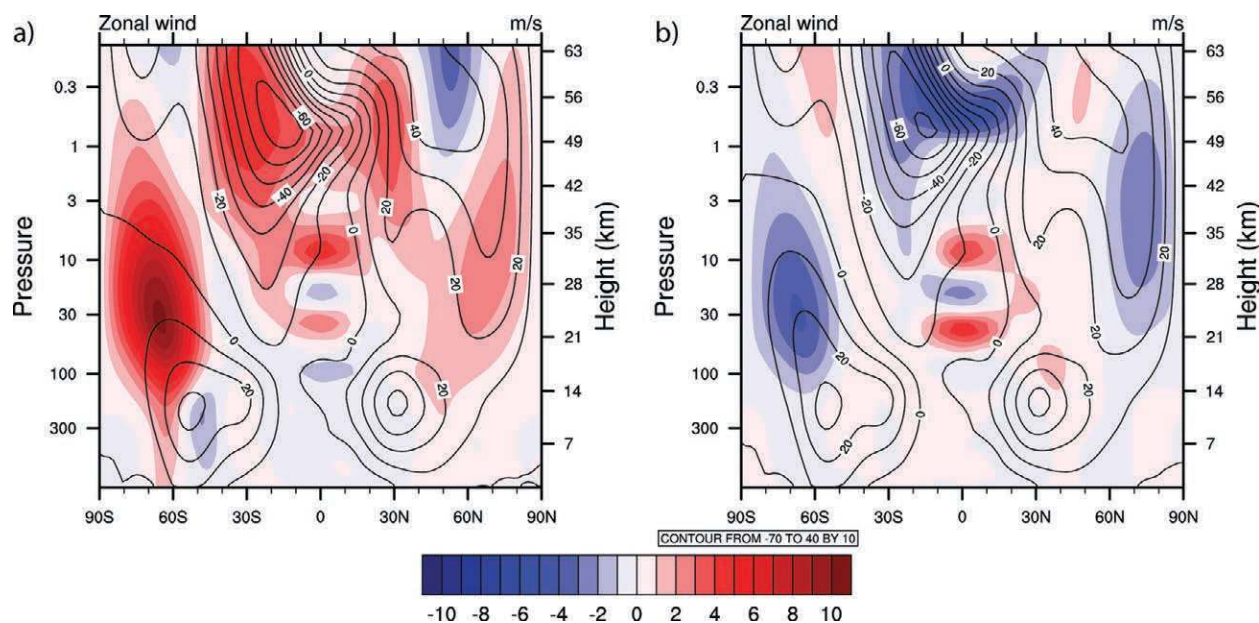


FIG. 7. Dec–Jan zonal-mean zonal winds (m s^{-1}): (a) 1960–79 average (line contours) and difference between means from 1986 to 2005 and from 1960 to 1979 (shaded contours) and (b) 2005–2024 average (line contours) and difference between means from 2032 to 2051 and from 2005 to 2024.

The area-integrated SMB falls sharply during the twenty-first century, reaching $-78 \pm 143 \text{ Gt yr}^{-1}$ for 2080–99 of the RCP 8.5 simulation (Fig. 10c). A negative SMB implies long-term decay of the ice sheet, even in the absence of iceberg calving. There is a modest precipitation increase as the climate warms, offset by a much greater increase in summer melting and runoff,

resulting in a lifting of the equilibrium line (the elevation where average accumulation and average ablation are equal) by about 500 m. Summer warming is largest in the north and west, in part because of sea ice losses along the coast, and smallest in the southeast, as a result of a slowdown in the Atlantic meridional overturning circulation (not shown).

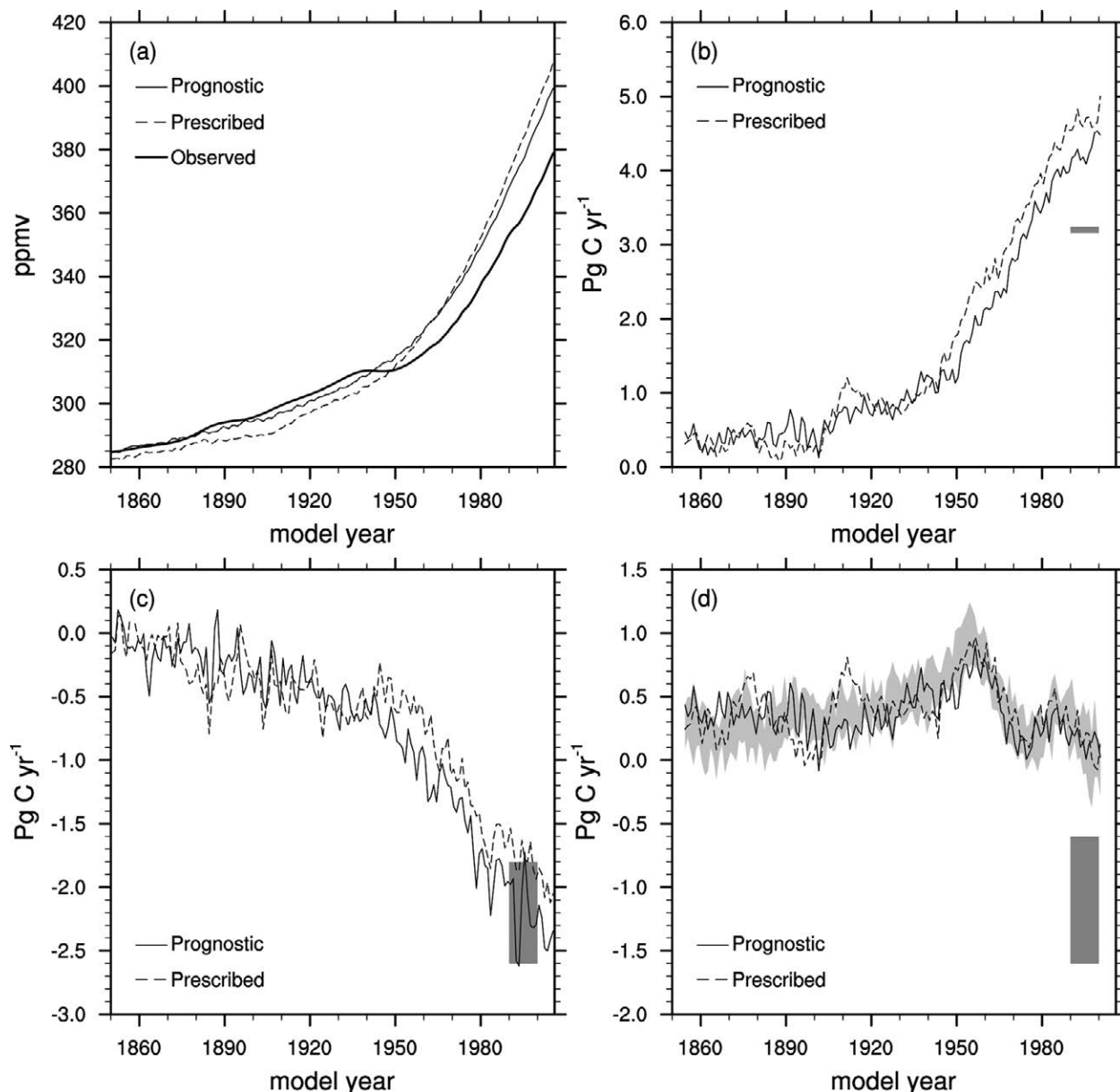


FIG. 8. Global annual-mean evolution of the carbon cycle in historical simulations (1850–2005) for (a) surface atmospheric CO_2 concentration; (b) net surface CO_2 flux, including fossil fuel emissions; (c) ocean surface CO_2 flux; and (d) land surface CO_2 flux. Solid lines show the case in which atmospheric CO_2 concentration is prognostic. Dashed lines show the prescribed CO_2 case in which the atmospheric CO_2 tracer is noninteractive; radiative transfer and biogeochemical fluxes are computed using observed CO_2 . A 10-point boxcar filter has been applied to the annual data in (b) and (d) to remove interannual variability. Dark shading denotes model/observational estimates from Canadell et al. (2007). Light shading in (d) denotes maximum and minimum filtered fluxes over seven CCSM4 twentieth-century ensemble members. Sign convention of the fluxes in each panel is positive up. [Adapted from Lindsay et al. (2013, manuscript submitted to *J. Climate*).]

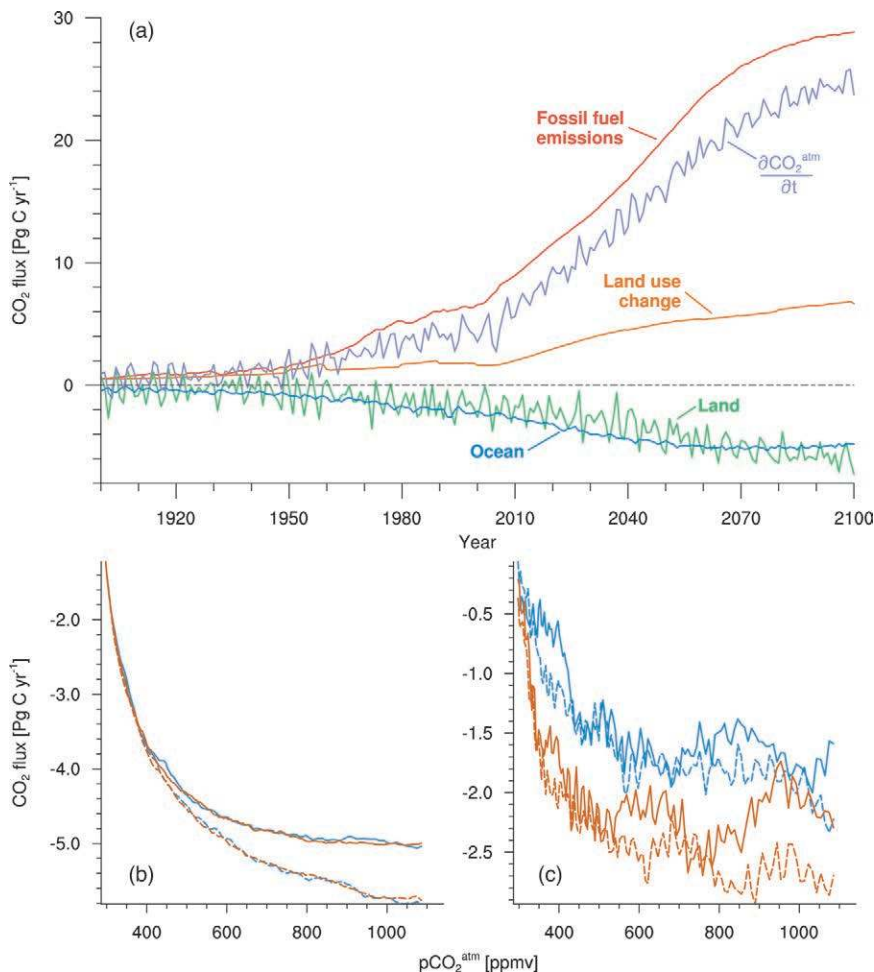


FIG. 9. (a) Temporal evolution of CO₂ sources, prognostic sinks, and the time tendency of atmospheric CO₂ for historical and RCP 8.5 conditions. Evolution of (b) ocean and (c) land CO₂ uptake under idealized 1% yr⁻¹ ramping CO₂ integrations. Solid lines show results from integrations in which both the radiative transfer and CO₂ flux calculations use the prescribed ramping CO₂ concentration. Dashed lines show results from simulations in which radiative CO₂ has been held constant at 1850 levels (thereby suppressing climate change), but the ramping CO₂ is used to compute land and ocean fluxes. Thus, the difference between the solid and dashed lines demonstrates the weakening of natural CO₂ sinks due to climate change. Blue lines in (b) and (c) show results from integrations in which surface N deposition was held constant; orange lines show results from integrations in which N deposition was increased to levels commensurate with RCP 8.5. Thus, the difference between the orange and blue lines demonstrates the effect of N limitation on CO₂ uptake. Sign convention for the fluxes in each panel is positive up.

SUMMARY AND FUTURE DIRECTIONS.

Computer models are powerful tools for meeting the intellectual challenge of understanding the climate and the Earth system, and they are the only scientific tool capable of integrating the myriad physical, chemical, and biological processes that determine past, present, and future climate. Models are also essential for testing and confirming understanding and for making predictions of use to society and policy makers.

The CESM is a community-wide project that is based at NCAR and is principally sponsored by the National Science Foundation and the U.S. Department of Energy. For many years, this project has been at the forefront of international efforts to understand and predict the behavior of Earth's climate. The development of this modeling system, moreover, occurs through strong partnership with scientists from universities, national laboratories, and other research organizations. Notably, expanded community involvement has enabled the transition from CCSM4 to CESM1, and the transition has allowed the investigation of new scientific problems, including those involved in adaptation and mitigation research.

A hallmark of the CESM project continues to be that there is community governance of all its activities. Accordingly, development and production objectives and priorities emanate directly from the community of scientists who participate in the management of the CESM project. This includes 12 CESM model development and application working groups (Fig. 11), which are teams of scientists that contribute

to the development of individual component models and application of the model to questions of interest. Membership is open to anyone, and a primary means of communication across groups is individuals participating in more than one. Each working group decides its own development and production priorities, subject to oversight by the CESM Scientific Steering Committee (SSC), which coordinates activities across working groups and is responsible for the

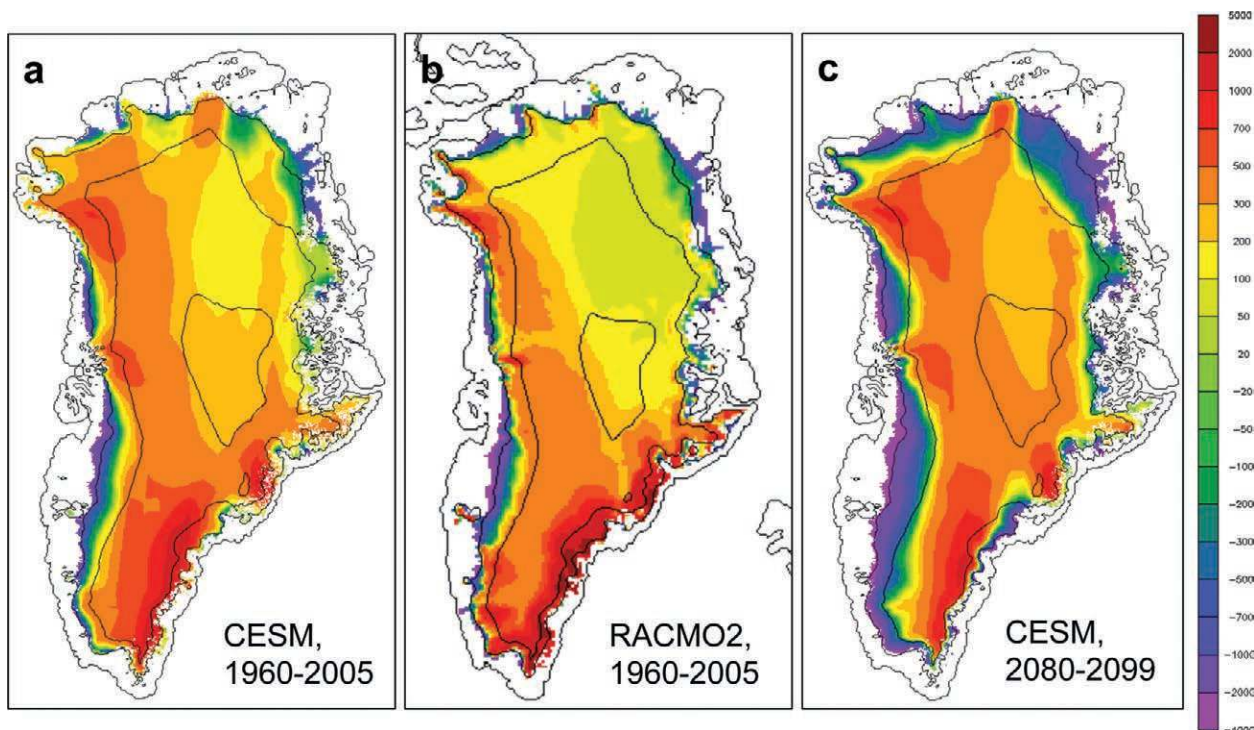


FIG. 10. Mean SMB (mm yr^{-1}) for the GrIS: (a) CESM1 (CISM), 1960–2005; (b) RACMO2 regional climate model, 1960–2005; and (c) CESM1 (CISM), 2080–99, using RCP 8.5 forcing. SMB is computed in the land model in 10 elevation classes per grid cell and then is downscaled to the ice sheet model grid.

overall development and release of the fully coupled model. An external CESM Advisory Board (CAB) assesses the progress and quality of the CESM activity, provides strategic advice on future CESM needs and plans, and provides help in building and expanding the CESM community (Fig. 11). All of these groups meet throughout the year, including an annual workshop in June that typically draws about 400 scientists and students from the U.S. and international research communities to Breckenridge, Colorado. More on the CESM management structure, the roles and responsibilities of the aforementioned groups, and meeting schedules can be found on the CESM web page (www.cesm.ucar.edu/).

The CESM project provides production simulations that have broad appeal across the climate science community and are thus made available for community access and analysis, following the CESM data management and data distribution plan (www.cesm.ucar.edu/management/docs/data.mgt.plan.2011.pdf). Examples are

simulations that contribute directly to coordinated national or international modeling activities, such as the CMIP5 simulations in Table 1, and “benchmark” simulations that document CESM components and new, coupled configurations of the model (e.g., control and transient simulations). In both examples,

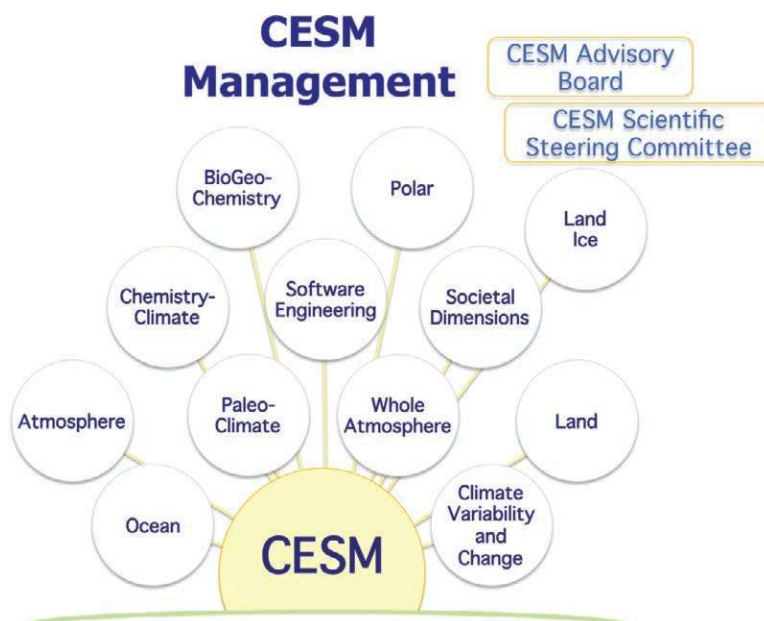


FIG. 11. Schematic of the CESM governance structure.

the project benefits directly from analysis and interpretation by the broader research community.

The outcome of community analysis often leads to new insights into model behavior and new development efforts, so that development and production activities are synergistic and sometimes become blurred. Current development priorities for CESM, identified by the 12 working groups and the scientific steering committee (SSC), can be broadly summarized into five overarching themes, briefly described next.

- *Coupling across components and understanding interactions.* A key attribute of CESM1 is the ability to simulate coupled interactions across different components of the climate system, including physical, chemical, and biological elements. Development work in this regard is focused on three main aspects: evaluating model performance against observations, which includes new diagnostics as well as coupled data assimilation techniques for systematic assessments of the modeling system; understanding the behavior of and refining the representation of physical processes; and expanding capabilities for coupling across components, such as ocean freshwater exchange as a result of the incorporation of a dynamic land ice model.
- *New parameterizations and processes.* To address the evolving scientific needs of the CESM community, progress demands that new processes be introduced and new parameterizations of existing processes be developed and tested. The incorporation of more Earth system components and efforts to run the CESM across a wider range of resolutions incur unique challenges for parameterization development. A considerable amount of development work is targeted at scale-aware parameterizations (e.g., Hurrell et al. 2009), including convection schemes, cloud processes, and boundary layer enhancements, that will enable the use of new model grids. Efforts are also directed at the simulation of cloud processes in the multiscale modeling framework (e.g., Randall et al. 2003), which embeds two-dimensional cloud-resolving physics within three-dimensional weather-scale physics (e.g., Khairoutdinov et al. 2008; Stan et al. 2010).

Overarching priorities are to improve the simulation of the radiative forcing of climate change by greenhouse gases (CO₂, ozone, and methane) and aerosols, as well as improve the treatment of the

feedback of climate change involving greenhouse gases, aerosols, clouds, and the cryosphere.

- *High-resolution and new dynamical cores.* With increases in computer resources, a societal need for climate information at more regional scales, and scientific questions associated with scale interactions and small-scale phenomena, important development efforts are focused on high-resolution simulations and new dynamical cores that enable these resolutions. It is now feasible, for instance, to consider coupling the following model components: a 1/4° atmosphere that resolves some organized convection; a 1/10° ocean that resolves the energetic mesoscale; a 1-km land to distinguish farms, natural lands, and neighborhoods; and sea ice with the resolution needed for cracking. These developments are occurring in close alignment to the requirement of performing efficiently with large processor counts on petascale-and-beyond computers. Even so, global integrations will be of limited duration, but regional grid refinement offers a trade-off between longer runs and even higher resolution in some components.

For the atmosphere, global resolutions up to 1/8° and regionally refined grids are being considered using a new spectral element (SE) dynamical core (Evans et al. 2012; Levy et al. 2013; see also Baer et al. 2006), as well as the Model for Prediction Across Scales (MPAS; Ringler et al. 2011). The complementary development of a high-resolution land model will enable coupled simulations on these grids, with sea ice to follow. The suitability of new atmospheric dynamical cores will be evaluated for the simulation of chemistry and in WACCM integrations when the resolution is incrementally increased. In the marine system, eddy-resolving physical models are beginning to include marine biogeochemistry, and an ocean-MPAS is being developed. Land ice models are incorporating new dynamical cores that resolve fast flow in ice streams and shelves with potential implications for ice sheet loss and sea level rise.

- *Addressing biases and other known shortcomings.* The simulation of historical climate in CESM1 is notably better than CCSM3. Gent et al. (2011) summarize the most noteworthy improvements, while more examples and details can be found in the CCSM4 papers in the *Journal of Climate* special collection. Moreover, as documented in this paper, CESM1 provides several new Earth system science capabilities over CCSM4, including the

ability to simulate the fully coupled carbon cycle and changes in the Greenland Ice Sheet, more fully quantify the effects of aerosols on climate, and the ability to examine the roles of chemistry and upper-atmospheric processes in climate variability and change. However, significant shortcomings remain to be addressed.

In the simulated atmosphere, for instance, issues such as the double intertropical convergence zone (ITCZ) and an excessive tropical water cycle remain, as in previous generations of the model (not shown). More generally, biases are present across CESM1 components and their influence propagates throughout the fully coupled system. Such is the case, for instance, in areas with too low ocean ventilation, creating hypoxic zones affecting the oceanic biogeochemical cycles and ultimately the carbon cycle.

- **Software development.** Software development covers three traditional and well-defined tasks: model testing, performance tuning, and debugging. These activities are essential for the efficient, reliable, and broad community use of CESM. In particular, a large number of combinations of model configurations and production machines are extensively tested to ensure reliability before being made available for community use. The need for debugging tests arises inevitably from systems' issues, or from new dynamic capabilities and parameterizations, processor layouts, and resolutions. Performance tuning is taking on added significance with the trend to higher-resolution simulations requiring very high processor counts.

In summary, a major objective for the CESM community is to more fully explore and document many of the new capabilities of the model. This includes novel representations of Earth system processes and their interconnections, and new developments in component models, including how they impact the coupled climate and climate sensitivity. The first version of CESM has not been fully characterized in the context of its representation of the past climate and its projections of future climate. Such characterization requires, for instance, much larger ensembles of simulations (than listed in Table 1) designed to characterize the spread of climate predictions generated by internal variability (e.g., Deser et al. 2012), the role of polar processes in determining climate sensitivity, and the role of patterns of oceanic surface temperature in generating atmospheric variability.

The key aim of the CESM project will continue to be providing the broader academic community a core modeling system for studies of past and current climate, and projections of future climate change. More specifically, the long-term goals of the CESM project are simple but ambitious. They are to develop and work continuously to improve a comprehensive ESM that is at the forefront of international efforts in modeling the climate system, including the best possible component models coupled together in a balanced, harmonious modeling framework; to make the model freely and readily available to, and usable by, the climate research community; to actively engage the community in the ongoing process of model development; to use the CESM to address important scientific questions about the climate system, including global change and interdecadal variability; and to use appropriate versions of the CESM for simulations in support of U.S. national and international policy decisions.

ACKNOWLEDGMENTS. We thank the three referees of the original submission. Their constructive comments and suggestions improved the manuscript considerably. We also thank Dr. Jin-ho Yoon and Adam Phillips for their help in the preparation of several figures, Miren Vizcaíno for providing output from CESM1(CISM) simulations, and William Sacks for software engineering support that made the CESM1(CISM) simulations possible. S. Ghan and P. Rasch were funded by the U.S. Department of Energy, Office of Science, Scientific Discovery through Advanced Computing (SciDAC) Program, and by the Office of Science Earth System Modeling Program. The Pacific Northwest National Laboratory is operated for the DOE by Battelle Memorial Institute under Contract DE-AC06-76RLO 1830.

Computing resources were provided by the Climate Simulation Laboratory at NCAR's Computational and Information Systems Laboratory (CISL), sponsored by the National Science Foundation and other agencies, and the Oak Ridge Leadership Computing Facility, located in the National Center for Computational Sciences at Oak Ridge National Laboratory, which is supported by the Office of Science (BER) of the Department of Energy under Contract DE-AC05-00OR22725. The CESM project is supported by the National Science Foundation and the Office of Science (BER) of the U.S. Department of Energy.

REFERENCES

- Allison, I., and Coauthors, 2009: The Copenhagen diagnosis: Updating the world on the latest climate

- science. University of New South Wales Climate Change Research Centre, 60 pp.
- Baer, F., H. Wang, J. J. Tribbia, and A. Fournier, 2006: Climate modeling with spectral elements. *Mon. Wea. Rev.*, **134**, 3610–3624.
- Bitz, C. M., and W. H. Lipscomb, 1999: An energy-conserving thermodynamic model of sea ice. *J. Geophys. Res.*, **104** (C7), 15 669–15 677.
- , K. M. Shell, P. R. Gent, D. A. Bailey, G. Danabasoglu, K. C. Armour, M. M. Holland, J. T. Kiehl, 2012: Climate sensitivity of the Community Climate System Model, version 4. *J. Climate*, **25**, 3053–3070.
- Blackmon, M. B., and Coauthors, 2001: The Community Climate System Model. *Bull. Amer. Meteor. Soc.*, **82**, 2357–2376.
- Bodas-Salcedo, A., and Coauthors, 2011: COSP: Satellite simulation software for model assessment. *Bull. Amer. Meteor. Soc.*, **92**, 1023–1043.
- Bougamont, M., J. L. Bamber, J. K. Ridley, R. M. Gladstone, W. Greuell, E. Hanna, A. J. Payne, and I. Rutt, 2007: Impact of model physics on estimating the surface mass balance of the Greenland Ice Sheet. *Geophys. Res. Lett.*, **34**, L17501, doi:10.1029/2007GL030700.
- Bourke, R. H., and R. P. Garrett, 1987: Sea ice thickness distribution in the Arctic Ocean. *Cold Reg. Sci. Technol.*, **13**, 259–280, doi:10.1016/0165-232X(87)90007-3.
- Bretherton, C. S., and S. Park, 2009: A new moist turbulence parameterization in the Community Atmosphere Model. *J. Climate*, **22**, 3422–3448.
- Briegleb, B. P., and B. Light, 2007: A delta-Eddington multiple scattering parameterization for solar radiation in the sea ice component of the Community Climate System Model. NCAR Tech. Note NCAR/TN-4721+STR, 100 pp.
- , G. Danabasoglu, and W. G. Large, 2010: An overflow parameterization for the ocean component of the Community Climate System Model. NCAR Tech. Note NCAR/TN-481+STR, 72 pp.
- Calvo, N., R. R. Garcia, D. R. Marsh, M. J. Miels, D. E. Kinnison, and P. J. Young, 2012: Reconciling modeled and observed temperature trends over Antarctica. *Geophys. Res. Lett.*, **39**, L16803, doi:10.1029/2012GL052526.
- Canadell, J. G., and Coauthors, 2007: Contributions to accelerating atmospheric CO₂ growth from economic activity, carbon intensity, and efficiency of natural sinks. *Proc. Natl. Acad. Sci. USA*, **104**, 18 866–18 870, doi:10.1073/pnas.0702737104.
- Castillo, C. K. G., S. Levis, and P. Thornton, 2012: Evaluation of the new CNDV option of the Community Land Model: Effects of dynamic vegetation and interactive nitrogen on CLM4 means and variability. *J. Climate*, **25**, 3702–3714.
- Collins, W. D., and Coauthors, 2006: The Community Climate System Model version 3 (CCSM3). *J. Climate*, **19**, 2122–2143.
- Collins, W. J., and Coauthors, 2011: Development and evaluation of an Earth-system model—HadGEM2. *Geosci. Model Dev*, **4**, 1051–1075, doi:10.5194/gmd-4-1051-2011.
- Craig, A. P., M. Vertenstein, and R. Jacob, 2012: A new flexible coupler for Earth system modeling developed for CCSM4 and CESM1. *Int. J. High Perform. Comput. Appl.*, **26**, 31–42, doi:10.1177/1094342011428141.
- Danabasoglu, G., R. Ferrari, and J. C. McWilliams, 2008: Sensitivity of an ocean general circulation model to a parameterization of near-surface eddy fluxes. *J. Climate*, **21**, 1192–1208.
- , W. G. Large, and B. P. Briegleb, 2010: Climate impacts of parameterized Nordic Sea overflows. *J. Geophys. Res.*, **115**, C11005, doi:10.1029/2010JC006243.
- , S. C. Bates, B. P. Briegleb, S. R. Jayne, M. Jochum, W. G. Large, S. Peacock, and S. G. Yeager, 2012: The CCSM4 ocean component. *J. Climate*, **25**, 1361–1389.
- D’Andrea, F., and Coauthors, 1998: Northern Hemisphere atmospheric blocking as simulated by 15 atmospheric general circulation models in the period 1979–1988. *Climate Dyn.*, **14**, 385–407.
- Deser, C., and Coauthors, 2012: ENSO and Pacific decadal variability in Community Climate System Model version 4. *J. Climate*, **25**, 2622–2651.
- Dunne, J. P., and Coauthors, 2012: GFDL’s ESM2 global coupled climate–carbon Earth system models. Part I: Physical formulation and baseline simulation characteristics. *J. Climate*, **25**, 6646–6665.
- Evans, K. J., P. H. Lauritzen, S. K. Mishra, R. B. Neale, M. A. Taylor, and J. J. Tribbia, 2012: AMIP simulation with the CAM4 spectral element dynamical core. *J. Climate*, **26**, 689–709.
- Eyring, V., and Coauthors, 2013: Long-term ozone changes and associated climate impacts in CMIP5 integrations. *J. Geophys. Res. Atmos.*, **118**, 5029–5060, doi:10.1002/jgrd.50316.
- Fetterer, F., K. Knowles, W. Meier, and M. Savoie, 2002: Sea ice index. National Snow and Ice Data Center, Boulder, CO, digital media. [Available online at http://nsidc.org/data/docs/noaa/g02135_seaice_index/.]
- Flanner, M. G., C. S. Zender, J. T. Randerson, and P. J. Rasch, 2007: Present-day climate forcing and response from black carbon in snow. *J. Geophys. Res.*, **112**, D11202, doi:10.1029/2006JD008003.
- Flato, G. M., 2011: Earth system models: An overview. *Wiley Interdiscip. Rev.*, 783–800.

- Fox-Kemper, B., R. Ferrari, and R. Hallberg, 2008: Parameterization of mixed layer eddies. Part I: Theory and diagnosis. *J. Phys. Oceanogr.*, **38**, 1145–1165.
- Friedlingstein, P., and C. Prentice, 2010: Carbon-climate feedbacks: A review of model and observation based estimates. *Curr. Opin. Environ. Sustainability*, **2**, 251–257.
- , and Coauthors, 2006: Climate–carbon cycle feedback analysis: Results from the C₄MIP model intercomparison. *J. Climate*, **19**, 3337–3353.
- Gent, P. R., and Coauthors, 2011: The Community Climate System Model version 4. *J. Climate*, **24**, 4973–4991.
- Gottelman, A., H. Morrison, and S. J. Ghan, 2008: A new two-moment bulk stratiform cloud microphysics scheme in the NCAR Community Atmosphere Model (CAM3). Part II: Single-column and global results. *J. Climate*, **21**, 3660–3679.
- , J. E. Kay, and K. M. Shell, 2012: The evolution of climate sensitivity and climate feedbacks in the Community Atmosphere Model. *J. Climate*, **25**, 1453–1469.
- Ghan, S., X. Liu, R. Easter, P. Rasch, J. Yoon, and B. Eaton, 2012: Toward a minimal representation of aerosols in climate models: Comparative decomposition of aerosol direct, semi-direct and indirect radiative forcing. *J. Climate*, **25**, 6461–6476.
- Giorgetta, M. A., and Coauthors, 2012: Climate change from 1850 to 2100 in MPI-ESM simulations for the Coupled Model Intercomparison Project 5. *J. Adv. Model. Earth Syst.*, in press, doi:10.1002/jame.20038.
- Holland, M. M., D. A. Bailey, B. P. Briegleb, B. Light, and E. Hunke, 2012: Improved sea ice shortwave radiation physics in CCSM4: The impact of melt ponds and aerosols on Arctic sea ice. *J. Climate*, **25**, 1413–1430.
- Hunke, E. C., and J. K. Dukowicz, 2002: The elastic–viscous–plastic sea ice dynamics model in general orthogonal curvilinear coordinates on a sphere—Incorporation of metric terms. *Mon. Wea. Rev.*, **130**, 1848–1865.
- , and W. H. Lipscomb, 2008: CICE: The Los Alamos sea ice model, documentation and software, version 4.0. Los Alamos National Laboratory Tech. Rep. LA-CC-06-012, 76 pp.
- Hurrell, J. W., G. A. Meehl, D. Bader, T. Delworth, B. Kirtman, and B. Wielicki, 2009: A unified modeling approach to climate system prediction. *Bull. Amer. Meteor. Soc.*, **90**, 1819–1832.
- Hurtt, G. C., S. Frolking, M. G. Fearon, B. Moore, E. Sheviliakova, S. Malyshev, S. W. Pacala, R. A. Houghton, 2006: The underpinnings of land-use history: Three centuries of global gridded land-use transitions, wood-harvest activity, and resulting secondary lands. *Global Change Biol.*, **12**, 1208–1229, doi:10.1111/j.1365-2486.2006.01150.x.
- Iacono, M. J., J. S. Delamere, E. J. Mlawer, M. W. Shephard, S. A. Clough, and W. D. Collins, 2008: Radiative forcing by long-lived greenhouse gases: Calculations with the AER radiative transfer models. *J. Geophys. Res.*, **113**, D13103, doi:10.1029/2008jd009944.
- Jahn, A., and Coauthors, 2012: Late-twentieth-century simulation of Arctic sea ice and ocean properties in the CCSM4. *J. Climate*, **25**, 1431–1452.
- Jayne, S. R., 2009: The impact of abyssal mixing parameterizations in an ocean general circulation model. *J. Phys. Oceanogr.*, **39**, 1756–1775.
- Jochum, M., G. Danabasoglu, M. Holland, Y.-O. Kwon, and W. G. Large, 2008: Ocean viscosity and climate. *J. Geophys. Res.*, **113**, C06017, doi:10.1029/2007JC004515.
- Kawase, H., T. Nagashima, K. Sudo, and T. Nozawa, 2011: Future changes in tropospheric ozone under representative concentration pathways (RCPs). *Geophys. Res. Lett.*, **38**, L05801, doi:10.1029/2010GL046402.
- Kay, J. E., M. M. Holland, and A. Jahn, 2011: Interannual to multi-decadal Arctic sea ice extent trends in a warming world. *Geophys. Res. Lett.*, **38**, L15708, doi:10.1029/2011GL048008.
- , and Coauthors, 2012a: Exposing global cloud biases in the Community Atmosphere Model (CAM) using satellite observations and their corresponding instrument simulators. *J. Climate*, **25**, 5190–5207.
- , M. M. Holland, C. M. Bitz, E. Blanchard-Wrigglesworth, A. Gettelman, A. Conley, and D. Bailey, 2012b: The influence of local feedbacks and northward heat transport on the equilibrium Arctic climate response to increased greenhouse gas forcing. *J. Climate*, **25**, 5433–5450.
- Khairoutdinov, M., C. DeMott, and D. Randall, 2008: Evaluation of the simulated interannual and subseasonal variability in an AMIP-style simulation using the CSU multiscale modeling framework. *J. Climate*, **21**, 413–431.
- Kucharik, C. J., and A. N. D. K. R. Brye, 2003: Integrated Biosphere Simulator (IBIS) yield and nitrate loss predictions for Wisconsin maize receiving varied amounts of nitrogen fertilizer. *J. Environ. Qual.*, **32**, 247–268.
- Kwok, R., and G. F. Cunningham, 2008: ICESat over Arctic sea ice: Estimation of snow depth and ice thickness. *J. Geophys. Res.*, **113**, C08010, doi:10.1029/2008JC004753.
- Lacis, A. A., and J. E. Hansen, 1974: A parameterization for the absorption of solar radiation in the Earth's atmosphere. *J. Atmos. Sci.*, **31**, 118–133.

- Lamarque, J.-F., and Coauthors, 2010: Historical (1850–2000) gridded anthropogenic and biomass burning emissions of reactive gases and aerosols: Methodology and application. *Atmos. Chem. Phys.*, **10**, 7017–7039, doi:10.5194/acp-10-7017-2010.
- , G. P. Kyle, M. Meinshausen, K. Riahi, S. J. Smith, D. P. van Vuuren, A. J. Conley, and F. Vitt, 2011: Global and regional evolution of short-lived radiatively-active gases and aerosols in the representative concentration pathways. *Climatic Change*, **109**, 191–212, doi:10.1007/s10584-011-0155-0.
- , and Coauthors, 2012: CAM-chem: Description and evaluation of interactive atmospheric chemistry in the Community Earth System Model. *Geosci. Model Dev.*, **5**, 369–411, doi:10.5194/gmd-5-369-2012.
- Lawrence, D. M., K. W. Oleson, M. G. Flanner, P. E. Thornton, S. C. Swenson, P. J. Lawrence, X. Zeng, Z.-L. Yang, S. Levis, K. Sakaguchi, G. B. Bonan, and A. G. Slater, 2011: Parameterization improvements and functional and structural advances in version 4 of the Community Land Model. *J. Adv. Model. Earth Syst.*, **3**, M03001, doi:10.1029/2011MS000045.
- , —, —, C. G. Fletcher, P. J. Lawrence, S. Levis, S. C. Swenson, and G. B. Bonan, 2012a: The CCSM4 land simulation, 1850–2005: Assessment of surface climate and new capabilities. *J. Climate*, **25**, 2240–2260.
- , A. G. Slater, and S. C. Swenson, 2012b: Simulation of present-day and future permafrost and seasonally frozen ground conditions in CCSM4. *J. Climate*, **25**, 2207–2225, doi:10.1175/JCLI-D-11-00334.1.
- Lawrence, P. J., and Coauthors, 2012: Simulating the biogeochemical and biogeophysical impacts of transient land cover change and wood harvest in the Community Climate System Model (CCSM4) from 1850 to 2100. *J. Climate*, **25**, 3071–3095.
- Levis, S., G. B. Bonan, E. Kluzek, P. E. Thornton, A. Jones, W. J. Sacks, and C. J. Kucharik, 2012: Interactive crop management in the Community Earth System Model (CESM1): Seasonal influences on land–atmosphere fluxes. *J. Climate*, **25**, 4839–4859.
- Levy, M. N., J. R. Overfelt and M. A. Taylor, 2013: A variable resolution spectral element dynamical core in the Community Atmosphere Model. Sandia National Laboratories Tech. Note SAND 2013-0697J, 25 pp.
- Lipscomb, W. H., J. Fyke, M. Vizcaíno, W. Sacks, J. Wolfe, M. Vertenstein, T. Craig, E. Kluzek, and D. Lawrence, 2013: Implementation and initial evaluation of the Glimmer Community Ice Sheet Model in the Community Earth System Model. *J. Climate*, in press, doi:10.1175/JCLI-D-12-00557.1.
- Liu, X., and Coauthors, 2012: Toward a minimal representation of aerosols in climate models: Description and evaluation in the Community Atmosphere Model CAM5. *Geosci. Model Dev.*, **5**, 709–739, doi:10.5194/gmd-5-709-2012.
- Marsh, D. R., M. J. Mills, D. E. Kinnison, J.-F. Lamarque, N. Calvo, and L. M. Polvani, 2013: Climate change from 1850 to 2005 simulated in CESM1(WACCM). *J. Climate*, in press, doi:10.1175/JCLI-D-12-00558.1.
- Meehl, G. A., and Coauthors, 2012: Climate system response to external forcings and climate change projections in CCSM4. *J. Climate*, **25**, 3661–3683.
- , and Coauthors, 2013: Climate change projections in CESM1(CAM5) compared to CCSM4. *J. Climate*, in press, doi:10.1175/JCLI-D-12-00572.1.
- Moore, J. K., S. C. Doney, and K. Lindsay, 2004: Upper ocean ecosystem dynamics and iron cycling in a global three-dimensional model. *Global Biogeochem. Cycles*, **18**, GB4028, doi:10.1029/2004GB002220.
- Morice, C. P., J. J. Kennedy, N. A. Rayner, and P. D. Jones, 2012: Quantifying uncertainties in global and regional temperature change using an ensemble of observational estimates: The HadCRUT4 data set. *J. Geophys. Res.*, **117**, D08101, doi:10.1029/2011JD017187.
- Morrison, H., and A. Gettelman, 2008: A new two-moment bulk stratiform cloud microphysics scheme in the NCAR Community Atmosphere Model (CAM3). Part I: Description and numerical tests. *J. Climate*, **21**, 3642–3659.
- Neale, R. B., and Coauthors, 2012: Description of the NCAR Community Atmosphere Model (CAM 5.0). NCAR Tech. Note TN-486, 274 pp.
- , J. Richter, S. Park, P. H. Lauritzen, S. J. Vavrus, P. J. Rasch, and M. Zhang, 2013: The mean climate of the Community Atmosphere Model (CAM4) in forced SST and fully coupled experiments. *J. Climate*, **26**, 5150–5168.
- Oleson, K. W., G. B. Bonan, J. Feddema, M. Vertenstein, and C. S. B. Grimmond, 2008: An urban parameterization for a global climate model. Part I: Formulation and evaluation for two cities. *J. Appl. Meteor. Climatol.*, **47**, 1038–1060.
- , and Coauthors, 2010: Technical description of version 4.0 of the Community Land Model (CLM). NCAR Tech. Note NCAR/TN-478+STR, 257 pp.
- Park, S., and C. S. Bretherton, 2009: The University of Washington shallow convection and moist turbulence schemes and their impact on climate simulations with the Community Atmosphere Model. *J. Climate*, **22**, 3449–3469.
- Pattyn, F., and Coauthors, 2008: Benchmark experiments for higher-order and full-Stokes ice sheet models (ISMIP-HOM). *Cryosphere*, **2**, 95–108.
- Pincus, R., H. W. Barker., and J.-J. Morcrette, 2003: A fast, flexible, approximation technique for computing

- radiative transfer in inhomogeneous cloud fields. *J. Geophys. Res.*, **108**, 4376, doi:10.1029/2002JD003322.
- Price, S. F., A. J. Payne, I. M. Howat, and B. E. Smith, 2011: Committed sea-level rise for the next century from Greenland ice sheet dynamics during the past decade. *Proc. Natl. Acad. Sci. USA*, **108**, 8978–8983.
- Randall, D., M. Khairoutdinov, A. Arakawa, and W. Grabowski, 2003: Breaking the cloud parameterization deadlock. *Bull. Amer. Meteor. Soc.*, **84**, 1547–1564.
- Riahi, K., S. Rao, V. Krey, C. Cho, V. Chirkov, G. Fischer, G. Kindermann, N. Nakicenovic, and P. Rafai, 2011: RCP 8.5—A scenario of comparatively high greenhouse gas emissions. *Climatic Change*, **109**, 33–57, doi:10.1007/s10584-011-0149-y.
- Rignot, E., I. Velicogna, M. R. van den Broeke, A. Monaghan, and J. Lenaerts, 2011: Acceleration of the contribution of the Greenland and Antarctic Ice Sheets to sea level rise. *Geophys. Res. Lett.*, **38**, L05503, doi:10.1029/2011GL046583.
- Ringler, T. D., D. Jacobsen, M. Gunzburger, L. Ju, M. Duda, and W. Skamarock, 2011: Exploring a multiresolution modeling approach within the shallow-water equations. *Mon. Wea. Rev.*, **139**, 3348–3368.
- Rothrock, D. A., 1975: The energetics of the plastic deformation of pack ice by ridging. *J. Geophys. Res.*, **80** (33), 4514–4519.
- Rutt, I., M. Hagdorn, N. J. R. Hulton, and A. J. Payne, 2009: The Glimmer Community Ice Sheet Model. *J. Geophys. Res.*, **114**, F02004, doi:10.1029/2008JF001015.
- Sacks, W. J., B. I. Cook, N. Buening, S. Levis, and J. H. Helkowski, 2009: Effects of global irrigation on the near-surface climate. *Climate Dyn.*, **33**, 159–175, doi:10.1007/s00382-008-0445-z.
- Scaife, A. A., T. Woollings, J. Knight, G. Martin, and T. Hinton, 2010: Atmospheric blocking and mean biases in climate models. *J. Climate*, **23**, 6143–6152.
- Smith, R. D., and Coauthors, 2010: The Parallel Ocean Program (POP) reference manual: Ocean component of the Community Climate System Model (CCSM) and Community Earth System Model (CESM). Los Alamos National Laboratory Tech. Rep. LAUR-10-01853, 141 pp. [Available online at www.cesm.ucar.edu/models/cesm1.0/pop2/doc/sci/POPRefManual.pdf.]
- SPARC CCMVal, 2010: SPARC report on the evaluation of chemistry–climate models. V. Eyring, T. G. Shepherd, and D.W. Waugh, Eds., SPARC Rep. 5, WCRP-132, WMO/TD-1526, 434 pp. [Available online at www.sparc-climate.org/publications/sparc-reports/.]
- Stan, C., M. Khairoutdinov, C. A. DeMott, V. Krishnamurthy, D. M. Straus, D. A. Randall, J. L. Kinter III, and J. Shukla, 2010: An ocean-atmosphere climate simulation with an embedded cloud resolving model. *Geophys. Res. Lett.*, **37**, L01702, doi:10.1029/2009GL040822.
- Stroeve, J. C., V. Kattsov, A. Barrett, M. Serreze, T. Pavlova, M. Holland, and W. N. Meier, 2012: Trends in Arctic sea ice extent from CMIP5, CMIP3 and observations. *Geophys. Res. Lett.*, **39**, L16502, doi:10.1029/2012GL052676.
- Taylor, K. E., R. J. Stouffer, and G. A. Meehl, 2012: An overview of CMIP5 and the experiment design. *Bull. Amer. Meteor. Soc.*, **93**, 485–498.
- Thompson, D. W. J., and S. Solomon, 2005: Recent stratospheric climate trends as evidence in radiosonde data: Global structure and tropospheric linkages. *J. Climate*, **18**, 4785–4795.
- Thonicke, K., S. Venevsky, S. Sitch, and W. Cramer, 2001: The role of fire disturbance for global vegetation dynamics: Coupling fire into a Dynamic Global Vegetation Model. *Global Ecol. Biogeogr.*, **10**, 661–667.
- Thorndike, A. S., D. A. Rothrock, G. A. Maykut, and R. Colony, 1975: The thickness distribution of sea ice. *J. Geophys. Res.*, **80** (33), 4501–4513.
- Thornton, P. E., J.-F. Lamarque, N. A. Rosenbloom, and N. M. Mahowald, 2007: Influence of carbon-nitrogen cycle coupling on land model response to CO₂ fertilization and climate variability. *Global Biogeochem. Cycles*, **21**, GB4018, doi:10.1029/2006GB002868.
- , S. Doney, K. Lindsay, J. K. Moore, N. Mahowald, J. Randerson, I. Fung, J. F. Lamarque, J. Feddesma, and Y.-H. Lee, 2009: Carbon-nitrogen interactions regulate climate-carbon cycle feedbacks: Results from an atmosphere-ocean general circulation model. *Biogeosciences*, **6**, 2099–2120.
- van Angelen, J. H., J. T. M. Lenaerts, S. Lhermitte, X. Fettweis, P. Kuipers Munneke, M. R. van den Broeke, and E. van Meijgaard, 2012: Sensitivity of Greenland Ice Sheet surface mass balance to surface albedo parameterization: A study with a regional climate model. *Cryosphere Discuss.*, **6**, 1531–1562.
- van Vuuren, D. P., M. G. den Elzen, P. L. Lucas, B. Eickhout, B. J. Strengers, B. van Ruijven, S. Wonink, and R. van Houdt, 2007: Stabilizing greenhouse gas concentrations at low levels: An assessment of reduction strategies and costs. *Climatic Change*, **81**, 119–159, doi:10.1007/s10584-10006-19172-10589.
- Vavrus, S. J., M. M. Holland, A. Jahn, D. A. Bailey, and B. A. Blazey, 2012: Twenty-first-century Arctic climate change in CCSM4. *J. Climate*, **25**, 2696–2710.
- Vizcaíno, M., W. H. Lipscomb, W. J. Sacks, J. H. van Angelen, B. Wouters, and M. R. van den Broeke, 2013a: Greenland surface mass balance as simulated by the Community Earth System Model. Part I: Model evaluation and 1850–2005 results. *J. Climate*, in press, doi:10.1175/JCLI-D-12-00615.1.

- Worden, H., K. Bowman, J. Worden, A. Eldering, and R. Beer, 2008: Satellite measurements of the clear-sky greenhouse effect from tropospheric ozone. *Nat. Geosci.*, **1**, 305–308, doi:10.1038/ngeo182.
- Yeager, S., A. Karspeck, G. Danabasoglu, J. Tribbia, and H. Teng, 2012: A decadal prediction case study: Late twentieth-century North Atlantic ocean heat content. *J. Climate*, **25**, 5173–5189.
- Zender, C. S., H. Bian, and D. Newman, 2003: Mineral Dust Entrainment and Deposition (DEAD) model: Description and 1990s dust climatology. *J. Geophys. Res.*, **108**, 4416, doi:10.1029/2002JD002775.
- Zhang, M. H., and Coauthors, 2005: Comparing clouds and their seasonal variations in 10 atmospheric general circulation models with satellite measurements. *J. Geophys. Res.*, **110**, D15S02, doi:10.1029/2004JD005021.